J Therm Anal Calorim (2012) 110:1217–1223
DOI 10.1007/s10973-011-2101-9

The use of TG/DSC–FT-IR to assess the effect of Cr sorption on struvite stability and composition

Ashaki A. Rouff

Received: 29 October 2011 / Accepted: 18 November 2011 / Published online: 9 December 2011

Abstract Struvite ($MgNH_4PO_4 \cdot 6H_2O$; MAP) can be recovered from animal and human wastes for use as fertilizer. This encourages the sustainable use of phosphorus (P), closing the human P cycle. The toxic metalloid chromium (Cr) is a common component of wastes, and can substitute for P in geochemical and biological systems. Thus, its sorption to, and effect on the stability and composition of recovered MAP requires assessment. MAP precipitated from solutions with 1–100 μM Cr(III) had higher Cr loadings compared to those reacted in the presence of Cr(VI), indicative of higher sorption affinity of the lower oxidation state. Simultaneous thermal analysis of unreacted MAP revealed an endothermic peak at 126 ± 0.5 °C by DSC with a mass loss of 52.9% by TG. Sorption of Cr produced minimal effects on the transition temperature and overall mass loss. The inflection in the TG curve indicated that Cr increased the temperature of maximum decomposition, but also the mass loss at this point. Combining TG results with FT-IR spectra revealed that for initial concentrations of 10–50 μM Cr(III) and 1–5 μM Cr(VI), NH_4^+ was added, and H_2O(s) lost from the MAP structure. The change in composition was consistent with substitution of Cr(III) or Cr(VI) into the MAP structure. The TG/DSC–FT-IR technique confirmed that Cr contamination affects the MAP composition and may accelerate the release of nutrients upon mineral decomposition. This has implications for the use of MAP fertilizers and subsequent cycling of P and contaminants in agricultural systems.

Keywords Struvite · Chromium · TG · DSC · FT-IR

A. A. Rouff (✉)
School of Earth and Environmental Sciences, Queens College, CUNY, 65-30 Kissena Blvd., Flushing, NY 11367, USA
e-mail: Ashaki.Rouff@qc.cuny.edu

Introduction

Phosphorus is essential to all life. It is also a limited natural resource, the cycling of which is accelerated by human activity due to its use as fertilizer. With diminishing geologic P reserves, and an ever increasing global population, P lost in the human cycle needs to be recouped [1]. The biomineral struvite ($MgNH_4PO_4 \cdot 6H_2O$; MAP) can help to close the P cycle as MAP recovered from human and animal wastes and wastewater has been targeted as an alternate, sustainable source of fertilizer [2–4]. This takes advantage of the spontaneous precipitation of MAP during some wastewater treatment processes [4–7], the ability to oversaturate and precipitate MAP from human urine [8, 9], and the formation of MAP from sewage sludge and animal waste during biofuels production [4, 10]. The recovery and repurposing of MAP from these sources would utilize P that is already a part of the human cycle, which is otherwise lost to the environment, often resulting in pollution. This in turn would encourage sustainable use of P, and aid in the conservation of non-renewable geologic P reserves [11].

Various wastes and wastewaters contain several contaminants. These include the metalloid chromium (Cr), which has been detected in MAP precipitated from both sewage sludge effluent and urine [12, 13]. This is concerning as Cr can displace and follow the same pathways as P in both geochemical and biological systems, with toxic effects for plants and organisms. The solid reactivity and toxicity of Cr is contingent upon oxidation state, with Cr(III) relatively immobile in the presence of solids and less toxic compared to Cr(VI), which remains in solution and is easily transported [14]. Sorption of Cr with MAP may proceed by several mechanisms including substitution into the MAP mineral structure during crystallization,

adsorption to already precipitated MAP, or by precipitation of oversaturated Cr phases. These processes can alter the composition of MAP, influencing both the recovery process and the subsequent decomposition and release of nutrients. The total Cr content of MAP also requires consideration if this product is to be introduced to agricultural soils and crops.

Thermal analysis can be a powerful tool in the characterization of MAP, as structural water (H_2O(s)) and ammonium ions (NH_4^+) are readily evolved on heating. Previous studies using thermogravimetric analysis (TG) and differential thermal analysis (DTA) revealed endothermic transitions at ~80–250 °C associated with the progressive loss of volatiles from MAP [15–18]. Thermal analysis may also be useful in determining the effect of sorbed contaminants on mineral properties. For example, TG revealed increased mass loss for Cr(III)-substituted hydroxylapatite ($Ca_5(PO_4)_3OH$; HAP) due to incorporation of additional hydroxyl ions with Cr [19]. Thus, this is a viable approach for studying metal sorption, however, heretofore there are no documented thermoanalytical studies of Cr sorption, or that of any other metals, with MAP, due to limited prior geochemical interest in this mineral.

The current study combines TG and differential scanning calorimetry (DSC) with evolved gas analysis by Fourier transform infrared spectroscopy (FT-IR) to study Cr sorbed MAP. The hyphenated technique has been used to characterize a wide variety of materials [20–23]. For MAP this approach is effective as FT-IR can distinguish between evolved H_2O(g) and NH_3(g), which have similar molecular masses and cannot be identified by TG alone. Experiments were designed to precipitate MAP in the presence of either Cr(III) or Cr(VI) over a range of initial Cr concentrations. Results from TG/DSC–FT-IR were used to assess the effect of Cr on the both the stability and composition of MAP. Furthermore, the technique was used to propose potential mechanisms of Cr sorption with MAP. Results from this study demonstrate that Cr can contaminate MAP fertilizers, influencing the release, and thus cycling of P and contaminants in agricultural systems.

Materials and methods

Precipitation of MAP in the presence of Cr

Experiments were designed to assess the sorption of Cr with actively precipitating MAP. The required solution chemistry was calculated using the program PHREEQC [24] with the minteq.v4 database and MAP solubility values from the literature [25]. An initial MAP saturation index of 2 (log $\Omega_{MAP} = 2$) was used as this is known to result in the formation of a homogeneous MAP precipitate [26]. Stock solutions of $MgCl_2 \cdot 6H_2O$ and $(NH_4)_2HPO_4$ were prepared at concentrations so that when mixed, the desired MAP saturation would be attained. Prior to mixing either the Mg solution was spiked with Cr(III) as $Cr(NO_3)_3 \cdot 9H_2O$ or the PO_4 solution with Cr(VI) as Na_2CrO_4 for final Cr concentrations of 1–100 μM. Solutions were then reacted in the presence of 0.1 g L^{-1} MAP seed, and spontaneous precipitation allowed to proceed at pH 7.8 ± 0.2. All samples were prepared in duplicate. Blanks, without added Cr (0 μM), were included for each experiment. After 7 days, reacted solids were recovered by filtration and allowed to air dry for subsequent characterization. An aliquot of filtered solution was retained, and a small portion of solid was acid digested to determine final aqueous and solid Cr concentration, respectively, by inductively coupled plasma optical emission spectroscopy (ICP-OES) using a Perkin Elmer Optima DV5300 instrument.

X-ray diffraction

Selected solids were characterized by X-ray diffraction (XRD) using a Phillips XPert Pro instrument with a CuKα radiation source. Data were collected over a range of 5°–60° 2θ in 0.02 step sizes with integration times of 0.5 s. The experimental diffraction pattern for synthesized MAP was compared to the theoretical pattern derived from the literature [27].

Thermal analysis

All recovered solids were subject to TG/DSC–FT-IR analysis. For the hyphenated technique, a simultaneous thermal analyzer, Perkin Elmer STA 6000, was connected to a Spectrum 100 FT-IR using a gas transfer line and specially designed FT-IR cell. Approximately 30 mg of sample was placed in a ceramic crucible and heated at a rate of 10 °C min^{-1} over a range of 25–400 °C. The sample purge was dry N_2(g) with a flow rate of 20 mL min^{-1}. Evolved gases were transported through the transfer line, into the FT-IR cell, both of which were heated to 250 °C to prevent gas condensation. The FT-IR was configured to continuously collect background-corrected spectra over a wavenumber range of 600–4,000 cm^{-1} for the duration of the temperature program.

Results and discussion

Sorption of Cr by MAP

Results from ICP-OES analysis of aqueous and solid samples indicate notable differences in the affinity of Cr for MAP contingent upon oxidation state (Fig. 1). Removal of

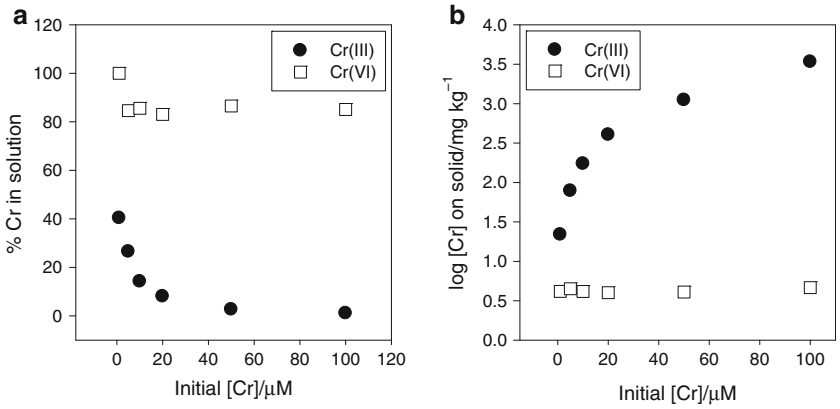

Fig. 1 Sorption of Cr(III) and Cr(VI) with MAP after 7 days reaction **a** percentage Cr remaining in solution and **b** final loading of Cr on the solid

both aqueous Cr(III) and Cr(VI) increases with initial concentration. The minimum final aqueous concentrations are 1 and 83% of the initial Cr(III) and Cr(VI), respectively (Fig. 1a). Commensurate with the trend for aqueous samples, the solid loadings of Cr(III), and more subtly, that of Cr(VI) increase with initial concentration (Fig. 1b). Significantly higher solid loadings for Cr(III) compared with Cr(VI), coupled with results from aqueous samples, indicates greater affinity of Cr(III) for MAP.

A high sorption affinity of Cr(III) for MAP, also compared to that for other phosphate minerals including HAP, has been observed previously [28]. For Cr(VI) samples, low loadings may be a result of competition between the dominant CrO_4^{2-}(aq) and HPO_4^{2-}(aq) species in solution for similar MAP sorption sites. In addition, sorption of CrO_4^{2-}(aq) may be inhibited by the predominantly negative surface charge of precipitating MAP at the reaction pH 7.8 ± 0.2 [29]. The highest Cr(III) solid concentrations may be due to precipitation of amorphous solids, such as $Cr(OH)_3$(am), which may accumulate at the MAP surface.

X-ray diffraction

Theoretical XRD patterns for MAP are quite variable depending on the geological or biological source, or method of synthesis. The highest intensity peaks at 14.5° and 30.5° 2θ are characteristic of MAP, and evident in the XRD pattern of the solid synthesized in the current study (Fig. 2). This confirms the formation of MAP using the chosen method of synthesis.

Thermal analysis of unreacted MAP

For unreacted MAP, DSC reveals an endothermic peak at 126.1 ± 0.5 °C with an onset temperature of 87 ± 0.5 °C (Fig. 3a). The transition is associated with significant mass loss from the sample as indicated by TG, and an increase in the absorbance in the FT-IR (Fig. 3a). The temperature-dependent FT-IR spectra reveal changes in absorbance

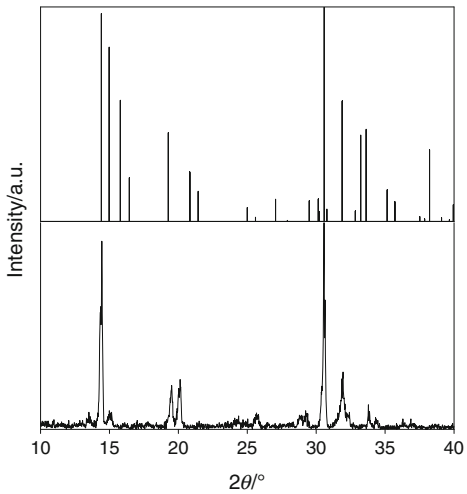

Fig. 2 XRD pattern for MAP synthesized in this study and diffraction lines for struvite from Ferraris et al. [27]

in the 1,300–2,000 cm^{-1} range, and at >3,500 cm^{-1}, characteristic of H_2O(g), and at ~1,000 cm^{-1}, due to NH_3(g) (Fig. 3b). Release of these gases is maximized near the endothermic transition, with continued release up to 200 °C. Additional NH_3(g) is evolved up to 300 °C. At the end of the heating program at 400 °C all volatiles are released from the sample with an overall mass loss of 52.9%. For the theoretical MAP composition, structural H_2O and NH_4^+ account for 50.9% of the mass. Thus, under the current conditions of MAP synthesis, a small fraction of additional volatiles appears to be associated with the structure.

Previous thermoanalytical studies indicated a multi-stage decomposition for MAP. For synthetic MAP, endothermic events at ~103 and 235 °C, and an exotherm at ~600 °C were associated with decomposition to the monohydrate ($NH_4MgPO_4 \cdot H_2O$), formation of an amorphous phase ($MgHPO_4$), and formation of the pyrophosphate ($Mg_2P_2O_7$) [15, 16]. Renal stones composed of MAP were also found to undergo endothermic and exothermic reactions within a range of 80–250 °C and 650–700 °C, respectively [17]. In the current study, the temperature

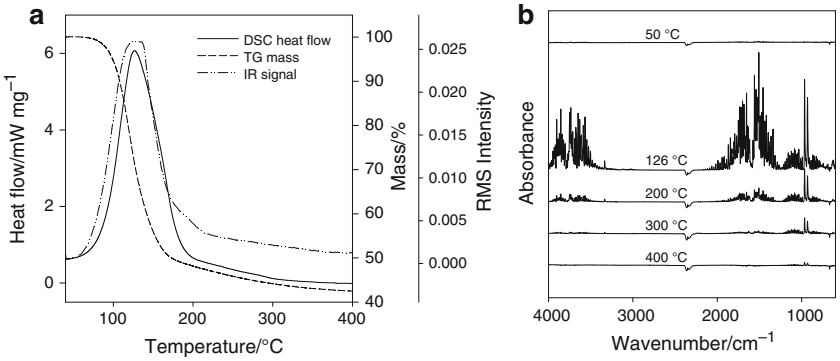

Fig. 3 TG/DSC–FT-IR results for unreacted MAP. **a** DSC heat flow, percentage mass loss by TG and absorbance in the FT-IR and **b** temperature-dependent FT-IR spectra

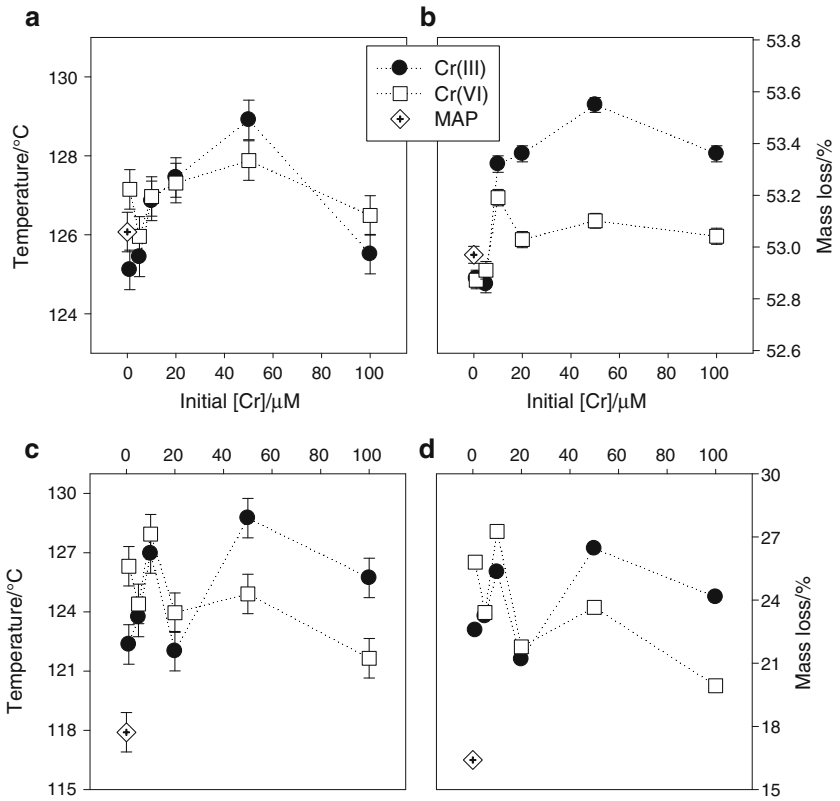

Fig. 4 DSC and TG results for Cr sorbed MAP compared to unreacted MAP. **a** Temperature of the endothermic transition, **b** overall mass loss from the sample, **c** temperature and **d** mass loss at the TG inflection point

range of MAP decomposition from the onset of the endothermic transition is ~87–300 °C, consistent with results for both synthetic and biogenic MAP. Slight differences in the temperature of the primary endothermic peak and the absence of a second distinct endothermic peak can be accounted for by variations in the conditions of synthesis, analytical conditions, and volatile content of the MAP compared to previous study. The exothermic reaction at >600 °C was not explored as the readily evolved volatile content is more likely to be affected by Cr sorption.

Thermal analysis of Cr sorbed MAP

The effect of Cr sorption on the temperature of the endothermic transition and total mass loss from the sample was determined by the comparison to that of unreacted MAP (Fig. 4a, b). For MAP precipitated in the presence of aqueous Cr, the temperature of the endothermic peak is mostly within error, with a maximum at 50 μM Cr (Fig. 4a). The total mass loss from the sample is close to that of unreacted MAP, but is consistently higher for initial Cr concentrations >5 μM (Fig. 4b), with a greater effect of Cr(III) compared to Cr(VI).

The effect of Cr sorption can also be assessed by examining the inflection point in the TG curve. This feature is indicative of the greatest mass loss from the sample. The temperature of the inflection point and the accompanying mass loss increases significantly for Cr-reacted MAP compared to unreacted MAP (Fig. 4c, d). The effect is more pronounced compared to that observed for the

endothermic transition and overall sample mass loss (Fig. 4a, b). Results indicate that sorption of both Cr(III) and Cr(VI) shifts the temperature of maximum MAP mass loss to higher temperature. This temperature shift is also accompanied by an overall increase in mass loss from the sample. This effect is more pronounced for Cr(III) relative to Cr(VI) reacted MAP samples, particularly at higher initial Cr concentration. Results confirm that sorption of Cr affects the decomposition process, and thus the stability of MAP.

Volatile content of Cr sorbed MAP

Due to the similarity in molecular mass of $H_2O(g)$ and $NH_3(g)$, the relative fraction of these constituents in the sample cannot be determined by TG alone. Coupling TG with FT-IR allows the volatile content of the MAP substrate to be calculated. This is accomplished by correlating the relative peak areas of $H_2O(g)$ and $NH_3(g)$ in the FT-IR spectra with the mass loss from the TG curve at the relevant temperature. For unreacted MAP, the volatile content is calculated as 7.3 mol, close to the stoichiometric value of 7 mol of H_2O and NH_4^+, and likely within error (Table 1).

For all Cr sorbed MAP samples the total volatile contents are similar to that of unreacted MAP (Table 1), which is consistent with small variations in observed total mass loss for all samples (Fig. 4b). However, for some samples there are notable changes in the relative moles of $H_2O(g)$ and $NH_3(g)$ evolved compared to unreacted MAP. For Cr(III) samples with initial concentrations of 10–50 μM, and the 5 μM Cr(VI) sample, the $H_2O(g)$ evolved decreases, and that of $NH_3(g)$ increases by approximately 1 mol, relative to unreacted MAP. For the 1 μM Cr(VI) sample the decrease in the number of $H_2O(g)$ and increase in that of $NH_3(g)$ is ~2 mol. These changes in the volatile content of MAP in the presence of Cr may be indicative of substitution of Cr into the mineral structure. If this is the case, results further suggest that this substitution occurs over a limited concentration range for both Cr(III) and Cr(VI).

Mechanisms of Cr substitution

For solids in which no effect of Cr on the bulk MAP composition was observed, Cr sorption to the mineral surface may dominate. At 1–5 μM Cr(III) and 10–100 μM Cr(VI) adsorption may be the primary mechanism, with Cr retained in the near surface region of MAP. For 100 μM Cr(III), precipitation of amorphous Cr solids may be an additional mechanism of Cr removal from solution. For both adsorption and surface precipitation, as Cr is not incorporated into the MAP mineral structure, minimal effects on the MAP composition would be expected.

The 10–50 μM Cr(III) and 1–5 μM Cr(VI) samples, which show changes in volatile content indicate that Cr substitution into the MAP structure may be a dominant mechanism. The MAP structure is comprised of Mg $(H_2O)_6$ octahedra linked to NH_4^+ and PO_4^{3-} tetrahedra by hydrogen bonding [27]. It is anticipated that Cr(III), which forms cationic species in solution will substitute at the Mg(II) site, and that Cr(VI) anions will substitute for P(V). Thus, the volatile content of Cr sorbed MAP can be used to propose the mechanisms of substitution. Based on equilibrium solution chemistry calculations, the dominant aqueous species for Cr(III) and Cr(VI) are $Cr(OH)_2^+(aq)$ and $CrO_4^{2-}(aq)$, respectively. Assuming interaction of the aqueous species with the precipitating mineral, and taking into account the addition of NH_4^+, and the loss of $H_2O(s)$ from the structure from TG and FT-IR, the following substitutions are proposed:

Table 1 Moles of evolved $H_2O(g)$ and $NH_3(g)$ for synthesized MAP compared to theoretical MAP, and for Cr sorbed MAP as determined from combined TG and FT-IR analysis

MAP	Synthesized			Theoretical		
	H_2O	NH_3	Total	H_2O	NH_3	Total
	5.6	1.8	7.3	6.0	1.0	7.0
[Cr]	Cr(III)			Cr(VI)		
	H_2O	NH_3	Total	H_2O	NH_3	Total
1	5.6	1.7	7.3	3.2	4.3	7.4
5	5.6	1.7	7.3	4.6	2.8	7.4
10	4.8	2.6	7.4	6.0	1.3	7.3
20	4.9	2.6	7.4	5.8	1.5	7.3
50	4.8	2.7	7.4	5.5	1.8	7.3
100	5.9	1.5	7.4	5.8	1.6	7.3

$$Cr(OH)_2^{+} + NH_4^{+} = Mg(H_2O)^{2+} \quad (1)$$

$$CrO_4^{2-} + NH_4^{+} = PO_4^{3-} + Mg(H_2O)^{2+} \quad (2)$$

In (1) the Cr $(OH)_2^{+}$ cation substitutes for Mg^{2+} in the structure, with the incorporation of additional NH_4^{+} for charge balance. Water of crystallization (H_2O(s)) may be lost from the structure to accommodate the Cr species, with the Cr hydroxyl ions (OH^{-}) less susceptible to volatilization compared to structural H_2O(s). In (2) CrO_4^{2-} substitutes for PO_4^{3-} accompanied by the addition of NH_4^{+} and removal of Mg^{2+} for charge compensation. Once again to accommodate the additional ions, H_2O(s) is lost from the structure. At 1 μM Cr(VI) a third mechanism may occur:

$$HCrO_4^{-} + 2NH_4^{+} = PO_4^{3-} + 2Mg(H_2O)^{2+} \quad (3)$$

Though $HCrO_4^{-}$(aq) only represents ~3% of the aqueous species, if crystallizing MAP has a mostly negative surface charge [29], the sorption of this less negative species may be preferable compared to CrO_4^{2-}(aq). In turn, this may proceed when the absolute CrO_4^{2-}(aq) is sufficiently low to limit out competition by this ion, which may be the case at 5 μM Cr(VI). The required charge balance for substitution of the $HCrO_4^{-}$(aq) species as in (3) is commensurate with the volatile content observed for this sample. It should be noted that the solid Cr concentrations for these samples indicates that only a small fraction of Cr substitutes into the structure (≤4 mg/kg). This suggests that even low concentrations of substituted Cr can propagate significant changes in the MAP the composition.

Implications for MAP use as fertilizer

The use of MAP as a fertilizer has several advantages. The mineral can simultaneously deliver the macronutrients P and N, as well as the secondary nutrient Mg to deficient plants. In addition, MAP recovered from wastewater has proved effective in improving both the yield and P content of plants and crops compared to other P fertilizers [30, 31]. Also, MAP may act as a slow-release fertilizer, reducing leaching and thus the premature loss of nutrients in targeted systems [2, 32].

This research indicates that MAP can be contaminated with Cr during recovery from wastes, with greater association of Cr(III) relative to Cr(VI) with the solid. Relatively low concentrations of substituted Cr can affect the overall composition of MAP. Of concern is the substitution of Cr(VI) for P(V) in the MAP structure. This can be detrimental, as Cr in this oxidation state can displace and follow the same pathways as P in soils and biological systems, with toxic effects for plants and organisms. At all concentrations studied, sorbed Cr was found to affect the thermal properties of MAP. Surprisingly, the mineral appeared to be less susceptible to decomposition. However, at the point of maximum decomposition the mass loss was higher compared to unreacted MAP, suggesting accelerated release of nutrients when decomposition does occur. This can affect its predicted properties as a slow-release fertilizer, as the accelerated release of nutrients can increase the probability of leaching. This cannot only limit nutrient availability to targeted plants, but excessive P and N can act as pollutants in natural ecosystems.

Summary and conclusions

This study outlines a novel application of TG/DSC–FT-IR to study the effect of Cr sorption on the properties of MAP. Results from DSC and TG indicated that sorbed Cr had a minimal effect on both the endothermic transition and total mass loss compared to unreacted MAP. The most significant effect was observed at the inflection point in the TG which shifted to higher temperature and produced greater mass loss compared to unreacted MAP. This indicated that though Cr increased the temperature of maximum decomposition, the loss of volatiles was expedited. The effect of Cr(III) on the thermal properties of MAP was more pronounced than that of Cr(VI), likely due to higher solid reactivity of the former. The volatile content of Cr sorbed MAP was used to provide mechanistic details concerning the Cr sorption mechanism. A significant change in the compositions of selected samples was interpreted as substitution of Cr(III) for Mg(II) or Cr(VI) for P(V) in the MAP structure. For other Cr samples, adsorption or precipitation were likely the dominant mechanisms.

The hyphenated TG/DSC–FT-IR technique elucidated the effect of Cr sorption on the stability of MAP and the overall mineral composition, including the co-sorption and/or loss of species associated with the structure. Of note is that this approach provided mechanistic information at low Cr loadings that would preclude analysis by techniques such as X-ray absorption fine structure spectroscopy (XAFS). The findings predicted potential interactions between Cr and MAP during P recovery from Cr-bearing wastes. Both Cr(III) and Cr(VI) can contaminate MAP even at low initial concentrations, which can prove toxic to plants and organisms. In addition, sorbed Cr can accelerate the release of nutrients from MAP upon decomposition. These findings have implications for the use of MAP fertilizers and subsequent cycling of P and N in geochemical systems.

Acknowledgements Support for this project was jointly funded by The Professional Staff Congress and The City University of New York, PSC-CUNY Award No. 63304. Thanks to Evert Elzinga, Jeffrey Fitts, and Alain Plante whose comments improved this manuscript.

References

1. Elser J, Bennet E. A broken biogeochemical cycle. Nature. 2011;478:29–31.
2. de-Bashan LE, Bashan Y. Recent advances in removing phosphorus from wastewater and its future use as fertilizer (1997–2003). Water Res. 2004;38:4222–46.
3. Arakane M, Imai T, Murakami S, Takeuchi M, Ukita M, Sekine M, Higuchi T. Resource recovery from excess sludge by subcritical water combined with magnesium ammonium phosphate process. Water Sci Technol. 2006;54:81–6.
4. Ro KS, Cantrell K, Elliott D, Hunt PG. Catalytic wet gasification of municipal and animal wastes. Ind Eng Chem Res. 2007;46:8839–45.
5. Borgerding J. Phosphate deposits in digestion systems. J Water Pollut Control Fed. 1972;44:813–9.
6. Suzuki K, Tanaka Y, Osada T, Waki M. Removal of phosphate, magnesium and calcium from swine wastewater through crystallization enhanced by aeration. Water Res. 2002;36:2991–8.
7. Yi W, Lo KV, Mavinic DS, Liao PH, Koch F. The effects of magnesium and ammonium additions on phosphate recovery from greenhouse wastewater. J Environ Sci Health. 2005;40:363–74.
8. Escher BI, Wouter P, Suter MJF, Maurer M. Monitoring the removal efficiency of pharmaceuticals and hormones in different treatment processes of source-separated urine with bioassays. Environ Sci Technol. 2006;40:5095–101.
9. Ronteltap M, Maurer M, Hausherr R, Gujer W. Struvite precipitation from urine—influencing factors on particle size. Water Res. 2010;44:2038–46.
10. Peterson AA, Vogel F, Lachance RP, Fröling M, Antal MJ, Tester JW. Thermochemical biofuel production in hydrothermal media: a review of sub-and supercritical water technologies. Energy Environ Sci. 2008;1:32–65.
11. Childers DL, Corman J, Edwards M, Elser JJ. Sustainability challenges of phosphorus and food: solutions from closing the human phosphorus cycle. Bioscience. 2011;61:117–24.
12. Ronteltap M, Maurer M, Gujer W. The behaviour of pharmaceuticals and heavy metals during struvite precipitation in urine. Water Res. 2007;41:1859–68.
13. Uysal A, Yilmazel YD, Demirer GN. The determination of fertilizer quality of the formed struvite from effluent of a sewage sludge anaerobic digester. J Hazard Mater. 2010;181:248–54.
14. Fendorf SE. Surface reactions of chromium in soils and waters. Geoderma. 1995;67:55–71.
15. Abdelrazig BEI, Sharp JH. Phase changes on heating ammonium magnesium phosphate hydrates. Thermochim Acta. 1988;129:197–215.
16. Sarkar AK. Hydration/dehydration characteristics of struvite and dittmarite pertaining to magnesium ammonium phosphate cement systems. J Mater Sci. 1991;26:2514–8.
17. Afzal M, Iqbal M, Ahmad H. Thermal analysis of renal stones. J Therm Anal. 1992;38:1671–82.
18. Frost RL, Weier ML, Erickson KL. Thermal decomposition of struvite implications for the decomposition of kidney stones. J Therm Anal Calorim. 2004;76:1025–33.
19. Wakamura M, Kandori K, Ishikawa T. Influence of chromium(III) on the formation of calcium hydroxyapatite. Polyhedron. 1997;16:2047–53.
20. Zapata B, Balmaseda J, Fregoso-Israel E, Torres-García E. Thermo-kinetics study of orange peel in air. J Therm Anal Calorim. 2009;98:309–15.
21. Miller TW. Use of TG/FT-IR in material characterization. J Therm Anal Calorim. 2011;106:249–54.
22. Hu Q, Jin HL, Chen XA, Wang S. Thermal and FT-IR spectral studies of *N,N′*-diphenylguanidine. J Therm Anal Calorim. 2011. doi:10.1007/s10973-011-1948-0.
23. Jingyan S, Zhiyong W, Yuwen L, Cunxin W. Investigation of thermal behavior of enoxacin and its hydrochloride. J Therm Anal Calorim. 2011. doi:10.1007/s10973-011-1817-x.
24. Parkhurst DL, Appelo CAJ. User's guide to PHREEQC (version 2)—a computer program for speciation, batch-reaction, one-dimensional transport, and inverse geochemical calculations. U.S. Geological Survey Water-Resources Investigations Report 99-4259; 1999.
25. Ohlinger KN, Young TM, Schroeder ED. Predicting struvite formation in digestion. Water Res. 1998;32:3607–14.
26. Bouropoulos NC. Koutsoukos PG spontaneous precipitation of struvite from aqueous solutions. J Cryst Growth. 2000;213:381–8.
27. Ferraris G, Fuess H, Joswig W. Neutron diffraction study of MgNH4PO4.6H2O (struvite) and survey of water molecules donating short hydrogen bonds. Acta Crystallogr. 1986;B42:253–8.
28. Shashkova IL, Rat'ko AI, Kitikova NV. Removal of heavy metal ions from aqueous solutions by alkaline-earth metal phosphates. Colloids Surf A. 1999;160:207–15.
29. Le Corre KS, Valsami-Jones E, Hobbs P, Jefferson B, Parsons SA. Agglomeration of struvite crystals. Water Res. 2007;41:419–25.
30. González-Ponce R, García-López-de-Sá ME. Evaluation of struvite as a fertilizer: a comparison with traditional P sources. Agrochimica. 2007;51:301–8.
31. González-Ponce R, López-de-Sá EG, Plaza C. Lettuce response to phosphorus fertilization with struvite recovered from municipal wastewater. HortScience. 2009;44:426–30.
32. Rahman Md M, Liu YH, Kwag J-H, Ra CS. Recovery of struvite from animal wastewater and its nutrient leaching loss in soil. J Hazard Mater. 2011;186:2026–30.